

# Modeling of Non-Stationary Creep Processes under Multiple Loading Conditions by Taking into Account Damage Accumulation in a Structural Material

I. A. Volkov<sup>a,\*</sup>, L. A. Igumnov<sup>a,\*\*</sup>, D. N. Shishulin<sup>a,\*\*\*</sup>, and E. V. Boev<sup>a,\*\*\*\*</sup>

<sup>a</sup> National Research Lobachevsky State University of Nizhny Novgorod,  
Nizhny Novgorod, 603022 Russia

\*e-mail: pmptmvgavt@yandex.ru

\*\*e-mail: igumnov@mech.unn.ru

\*\*\*e-mail: shishulindn@gmail.ru

\*\*\*\*e-mail: e.boev87@mail.ru

Received October 1, 2021; revised October 9, 2021; accepted October 11, 2021

**Abstract**—The article considers the problem on assessing the kinetics of the stress-strain state and the process of damage accumulation in polycrystalline structural materials of units and assemblies of engineering objects, the operational impacts of which are characterized by a highly loaded state under the influence of non-stationary long-term thermal force loading, where the main degradation mechanism is material creep. A mathematical model is presented. It is based on the concepts of the mechanics of a damaged medium and makes it possible to describe processes during unsteady creep under complex loading conditions and the main hypotheses underlying the mathematical model. By comparing the results of a numerical simulation with experimental data, a proof of the applicability of the mathematical model for uniaxial and multiaxial sign-variable loading conditions is given.

**Keywords:** long-term strength, material creep, mathematical modeling, damaged medium mechanics, creep model parameters, experimental data and numerical simulation

**DOI:** 10.3103/S0025654422020224

## 1. INTRODUCTION

For critical objects of mechanical engineering that are operated under conditions of non-stationary thermal and force effects with long periodic exposures at high temperatures and levels of acting stresses, the degradation of the structural material as a result of creep becomes significant. The problem on determining the resource of such structures becomes much more complex under the influence of slowly sign-changing loading by taking into account the presence of structural stress concentrators, where an accurate description of the kinetics of the stress-strain state that is used as the basis for applying approaches to assessing accumulated damage during operation is required [1–5]. For a reasonable description of rheonomic deformation processes, it is necessary to use mathematical models that are able to describe the processes of creep and damage accumulation in a structural material under the influence of a non-stationary temperature field and complex disproportionate force loading.

The most of the existing studies dealing with the mathematical modeling of creep processes are based on the use of one-dimensional models that describe the process of creep of materials by using basically equivalent values of stresses and strains [5, 6]. Under conditions of alternating loading, models based on strain hardening are used [3, 5, 6]. However, when performing estimates of the behavior of structures under conditions of non-stationary loading, it is necessary to take into account the vector properties of the parameters of the creep process, the effect of material damage on the kinetics of the creep process, and it is necessary to take into account the effect of reverse creep during material unloading, which affects the kinetics of the creep strain tensor under alternating loading with long-term unloading. As a result, it is necessary to build more complex mathematical models that describe the kinetics of the creep process. Many researchers believe that the application of the concept of introducing internal state parameters into the mathematical model makes it possible to satisfactorily describe the kinetics of the creep process under unsteady loading. These models allow describing both the scleronomic (loading time-independent) and

reonomic (loading time-dependent) parts of inelastic deformations of structural materials and are convenient for analyzing acting stresses by taking into account the effect of material damage.

In this article, based on the works of domestic and foreign authors [1–12], a mathematical model of unsteady creep is developed and numerical studies of the process of high-temperature creep for Kh18N10T steel under uniaxial loading and for steel 304 under multiaxial loading are presented. Based on the comparison of numerical and experimental results, the reliability of the applied mathematical model of non-stationary creep has been assessed.

## 2. MATHEMATICAL MODEL

The mathematical model of the damaged medium includes: equations describing the viscoelastic behavior of the material and the kinetics of the process of damage accumulation, as well as the criterion for the destruction of the degrading material.

The model is based on the following provisions [5]:

- structural material has initial isotropy of properties;
- processes of deformation of structural materials are characterized by small deformations;
- yield surfaces and creep strain rates are determined by the Mises form;
- change in equipotential surfaces of creep strain rates is determined by the displacement of the coordinates of the center  $\rho_{ij}^c$  and the value of the radius  $c_c$ ;
- change in the yield surface is determined by the displacement of the coordinates of the center  $\rho_{ij}$  and the value of the radius  $C_p$ ;
- plasticity and creep strain rates are determined from the associated flow law;
- change in the volume of the material is elastic (plastic incompressibility  $e_{ii}^p = 0$  is assumed);
- degree of damage for the material is taken into account by the damage parameter  $\omega$ , which varies in the range  $\omega_0 \leq \omega \leq \omega_f$  ( $\omega_0$  is the initial level of damage of the material, and  $\omega_f$  is the critical value of damage, characterized by the formation of a macrocrack);
- influence of the degree of degradation on the processes of elastic and inelastic deformation of the structural material is carried out by introducing a degrading continuum of effective stresses  $\tilde{\sigma}_{ij}$ .

It is postulated that the components of the strain tensor  $e_{ij}$  and strain rate tensor  $\dot{e}_{ij}$  obey the additivity rule and are the sum of elastic strains  $e_{ij}^e, \dot{e}_{ij}^e$  and creep strains  $e_{ij}^c, \dot{e}_{ij}^c$ :

$$e_{ij} = e_{ij}^e + e_{ij}^c; \quad \dot{e}_{ij} = \dot{e}_{ij}^e + \dot{e}_{ij}^c, \quad i, j = 1, 2, 3.$$

The stress tensor is related to the elastic strain tensor by the thermoelasticity equations:

$$\begin{aligned} \sigma &= 3K[e - \alpha T], \quad \dot{\sigma} = 3K[\dot{e} - \dot{\alpha}T - \alpha\dot{T}] + \frac{\dot{K}}{K}\sigma, \\ \sigma'_{ij} &= 2Ge'_{ij}, \quad \dot{\sigma}'_{ij} = 2G\dot{e}'_{ij} + \frac{\dot{G}}{G}\sigma'_{ij}, \quad e'_{ij}{}^e = e'_{ij} - e_{ij}^c, \end{aligned} \quad (2.1)$$

where  $\sigma, e$  are the hydrostatic and  $\sigma'_{ij}, e'_{ij}$  are the deviatoric parts of the stress  $\sigma_{ij}$  and strain  $e_{ij}$  tensors, respectively;  $G(T)$  is the Young's modulus of the 2nd kind (shear),  $K(T)$  is the bulk modulus of elasticity,  $\alpha(T)$  is the coefficient of linear expansion with temperature change.

To describe the creep processes, we introduce in the stress space the equipotential creep surfaces  $F_c$  having a common center  $\rho_{ij}^c$  and different radii  $C_c$  determined by the current stress state:

$$F_c^{(k)} = S_{ij}^c S_{ij}^c - C_c^2 = 0, \quad S_{ij}^c = \sigma'_{ij} - \rho_{ij}^c, \quad k = 0, 1, 2, \dots, \quad (2.2)$$

$$\dot{e}_{ij}^c = \lambda_c \frac{\partial F_c^{(i)}}{\partial S_{ij}^c} \dot{\tau} = \lambda_c S_{ij}^c \dot{\tau}, \quad (2.3)$$

where  $\lambda_c$  corresponds to the current surface  $F_c^{(k)}$ , which determines the current stress state  $S_{ij}^c$ .

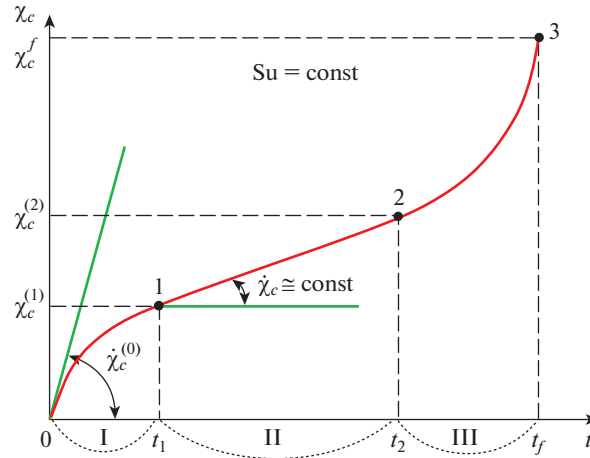


Fig. 1. Curve of the length of the trajectory of deformation during creep  $\chi_c$ .

A surface with radius  $\bar{C}_c$ , corresponds to zero creep velocity with a certain specified tolerance for the amount of creep strain on a certain time basis:

$$F_c^{(0)} = \bar{S}_{ij}^c \bar{S}_{ij}^c - \bar{C}_c^2 = 0, \quad \bar{S}_{ij}^c = \bar{\sigma}_{ij}^c - \rho_{ij}^c, \quad (2.4)$$

where  $\bar{S}_{ij}^c$  and  $\bar{\sigma}_{ij}^c$  are the sets of stress states corresponding to zero creep velocity.

$$\bar{C}_c = \bar{C}_c(\chi_c, T), \quad \dot{\chi}_c = \left( \frac{2}{3} \dot{e}_{ij}^c, \dot{e}_{ij}^c \right)^{1/2}, \quad \chi_c = \int_0^t \dot{\chi}_c dt; \quad \lambda_c = \lambda_c(\psi_c, T), \quad \lambda_c = \begin{cases} 0, & \psi_c \leq 0 \\ \lambda_c, & \psi_c > 0 \end{cases}, \quad (2.5)$$

where  $\bar{C}_c$  and  $\lambda_c$  are the functions of temperature  $T$  determined experimentally.

The evolution equation for changing the coordinates of the center of the creep surface has the form [13]:

$$\dot{\rho}_{ij}^c = g_1^c \dot{e}_{ij}^c - g_2^c \rho_{ij}^c \dot{\chi}_c - g_T^c \langle \dot{T} \rangle, \quad (2.6)$$

where  $g_1^c$  and  $g_2^c > 0$  are the kinematic hardening parameters and  $g_T^c$  is the temperature modulus.

Concretizing relation (2.3), the gradient law can be represented as:

$$\dot{e}_{ij}^c = \lambda_c \left( \frac{\sqrt{S_{ij}^c S_{ij}^c} - \bar{C}_c}{C_c} \right) S_{ij}^c \tau. \quad (2.7)$$

The expression for the length of the creep deformation trajectory has the following form:

$$\dot{\chi}_c = \sqrt{\frac{2}{3} \dot{e}_u^c} = \sqrt{\frac{2}{3}} \lambda_c (\sqrt{S_{ij}^c S_{ij}^c} - C_c) \tau. \quad (2.8)$$

The curve of the length of the deformation trajectory during creep  $\chi_c$  depending on the process time  $t$  at  $S_u^c = \text{const}$  has the form shown in Fig. 1.

On the curve  $\chi_c(t)$  (Fig. 1), three characteristic creep zones of the material can be distinguished:

- I. unsteady creep zone (0–1), where the creep strain rate  $\dot{\chi}_c$  decreases;
- II. steady creep zone (1–2), where the creep strain rate  $\dot{\chi}_c$  is approximately constant  $\dot{\chi}_c \cong \text{const}$ ;
- III. zone of active damage accumulation (2–3), where the creep strain rate  $\dot{\chi}_c$  constantly increases and the progressive effect of damage on the mechanical properties of the material begins.

The presence and length of zones I and II depend on the structural material and on the magnitude of the intensity of active stresses  $S_u^c$ .

The expression for  $\lambda_c^I$  in the first section of the creep curve can be represented as follows:

$$\lambda_c^I = \lambda_c^{(0)} \left( 1 - \frac{\chi_c}{\chi_c^{(1)}} \right) + \lambda_c^{(1)} \frac{\chi_c}{\chi_c^{(1)}}, \quad (2.9)$$

where  $\lambda_c^{(0)}$ ,  $\lambda_c^{(1)}$  are the values of the parameter  $\lambda_c$  at the points “0” and “1” on the first part of the creep curve of the material (see Fig. 1).

On the third section that is prior destruction, we have:

$$\lambda_c^{III} = \lambda_c^{II}(\omega), \quad (2.10)$$

where  $\omega$  is the amount of damage.

Relations (2.1)–(2.10) make it possible to simulate creep processes under nonisothermal nonstationary loading and describe the stages of unsteady and steady creep rates.

Constitutive relations (2.1)–(2.10), which describe the process of nonstationary nonisothermal creep, have been developed as a system of “embedded” mathematical models. By excluding from the equations the parameters (equalizing to zero) responsible for certain creep deformation effects, one can obtain particular mathematical models used in solving simple problems.

Damage affects the physical and mechanical properties at the stage of its development and active merging of scattered discontinuities in the volume of the structural material. To take into account the damage, effective stresses, which are defined as follows, are used:

$$\tilde{\sigma}'_{ij} = F_1(\omega) \sigma'_{ij} = \frac{G}{\tilde{G}} \sigma'_{ij}, \quad \tilde{\sigma} = F_2(\omega) \sigma = \frac{K}{\tilde{K}} \sigma, \quad (2.11)$$

where  $\tilde{G}$ ,  $\tilde{K}$  are the effective moduli of elasticity determined by the McKenzie formulas [13, 15]:

$$\tilde{G} = G(1 - \omega) \left[ 1 - \frac{(6K + 12G)}{(9K + 8G)} \omega \right], \quad \tilde{K} = 4GK(1 - \omega) / (4G + 3K\omega). \quad (2.12)$$

The effective internal variables  $\tilde{\rho}_{ij}^p$ ,  $\tilde{\rho}_{ij}^c$  are defined in a similar way:

$$\tilde{\rho}_{ij}^p = F_1(\omega) \rho_{ij}^p = \frac{G}{\tilde{G}} \rho_{ij}^p, \quad \tilde{\rho}_{ij}^c = F_1(\omega) \rho_{ij}^c = \frac{G}{\tilde{G}} \rho_{ij}^c. \quad (2.13)$$

When developing the constitutive relations for the kinetics of damage accumulation, it is assumed that the process of damage accumulation conditionally consists of two stages: the first stage is accompanied by the nucleation of discontinuities (micropores, microcracks), the second stage is the development and active merging of scattered discontinuities. The kinetic equation for damage accumulation in structural materials is taken in the simplest form of products of functions of internal parameters that affect the damage accumulation rate:

$$\dot{\omega} = f_1(\beta) f_2(\omega) f_3(W_c) f_4(\dot{W}_c). \quad (2.14)$$

In (2.14), the functions  $f_i$  make it possible to take into account the dependence of the damage accumulation rate  $\dot{\omega}$  on the following parameters of the deformation process:

- type of stress state—function  $f_1(\beta)$ ;
- current level of accumulated damage—function  $f_2(\omega)$ ;
- current value of the absorbed energy used for the formation of discontinuities (micropores and microcracks)—function  $f_3(W_c)$ ;
- current rate of change of absorbed energy  $W_c$ —function  $f_4(\dot{W}_c)$ .

$$f_1(\beta) = \exp(-k\beta), \quad f_2(\omega) = \begin{cases} 0, & W_c \leq W_c^a \\ c \cdot \omega^{-1/3} (1 - \omega)^{-2.3}, & W_c > W_c^a \end{cases}, \quad (2.15)$$

$$-f_3(W_c) = \frac{W_c - W_c^a}{W_c^f - W_c^a}, \quad f_4(\dot{W}_c) = \dot{W}_c / W_c^f, \quad \dot{W}_c = \rho_{ij}^c \dot{\epsilon}_{ij}^c, \quad W_c = \int_0^t \dot{W}_c dt. \quad (2.16)$$

Equations (2.15) and (2.16) have the following notations:

**Table 1.** Physical and mechanical characteristics and material parameters of the MDM model for Kh18N10T stainless steel

$T, ^\circ\text{C}$	$K, \text{MPa}$	$G, \text{MPa}$	$\bar{C}_c, \text{MPa}$	$\lambda_c^{(0)}, 1/\text{MPa h}$	$\lambda_c^{(1)}, 1/\text{MPa h}$	$g_1^c, \text{MPa}$	$g_2^c$	$W_c^f, \text{MJ/m}^3$	$W_c^a, \text{MJ/m}^3$	$\chi_c^{(1)}$
850	62855	29010	17	0.00011	0.00011	19000	224	4.7	0.3	0.03

–  $\beta$  is the “stiffness” parameter of the stress state ( $\beta = \sigma/\sigma_u$ );

–  $W_c^a$  is the value of the absorbed energy  $W_c$  at the end of the stage of nucleation of scattered discontinuities under creep conditions;

–  $W_c^f$  is the value of the absorbed energy corresponding to the formation of a macrocrack under creep conditions;

–  $c$  is the integration constant of Eq. (2.15).

The stage of development and merging of discontinuities in the structural material leads to the achievement of the level of accumulated damage of a critical value.

$$\omega = \omega_f \leq 1. \tag{2.17}$$

According to the given history of change in time for thermal and mechanical loading with joint integration of the equations describing the viscoelastic behavior (2.1)–(2.10) and the kinetics of damage accumulation (2.14)–(2.16), the resource of structural elements of engineering objects is determined under the conditions of the creep process in structural materials.

### 3. NUMERICAL RESULTS

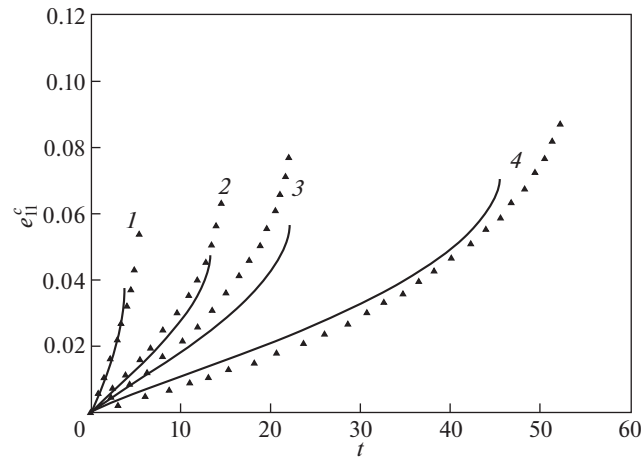
As part of the assessment of the reliability of the mathematical model by numerical simulation of creep processes in the uniaxial formulation of the problem for Kh18N10T steel, creep curves were numerically simulated at stress intensity levels  $\sigma_{11} = 40, 50, 60$  and  $80 \text{ MPa}$  and temperature  $T = 850^\circ\text{C}$ . The experimental basis for comparing numerical studies was the study [14], where the creep curves of the specified steel were given under identical loading conditions. Table 1 shows the physical and mechanical characteristics and parameters of the thermal creep model for Kh18N10T steel.

Figure 2 shows creep curves at temperature  $T = 850^\circ\text{C}$  and stress levels  $\sigma_{11} = 40, 50, 60$  and  $80 \text{ MPa}$ . The solid lines show the results of numerical simulation, and the dotted lines show the corresponding experimental results. One can see the qualitative and quantitative agreement between the experimental and calculated data.

As a part of the assessment of the reliability of the mathematical model of thermal creep under multi-axial loading, numerical studies of the creep process of steel 304 at a temperature of  $650^\circ\text{C}$  under biaxial loading were carried out. Experimental studies under biaxial loading laws for this steel were given in [7] and were performed on tubular laboratory samples. The tests were carried out at a constant temperature and periodic changes in the principal axes of the stress tensor (Fig. 4). In the tests, thin-walled tubular samples with an outer diameter of  $d = 21 \pm 0.05\text{mm}$ , a wall thickness of  $h = 1 \pm 0.05\text{mm}$  and a working length of  $l = 98\text{mm}$  were used. Figure 3 presents the comparison of the numerical results and experimental data under uniaxial loading of the specified steel for three levels of acting stresses ( $\sigma_{11} = 117.7; 137.3$  and  $156.9 \text{ MPa}$ ).

For testing under conditions of combined action of normal and shear components of stress and creep strain tensors, an axial force and torque were applied to the specimen in accordance with the established loading law. Each cycle of repeated multi-axial loading consisted of pure torsion  $\bar{\sigma}_A$  in  $t_{uac}^*$  with complete unloading and combined tension with torsion  $\bar{\sigma}_B$  in  $t_{uac}^*$  with unloading. The vectors  $\bar{\sigma}_A$  and  $\bar{\sigma}_B$  have the same value in different directions ( $\theta$  is the angle between the vectors, see Fig. 4). Such a loading cycle was repeated 5 times at  $t^* = 8 \text{ h}$  and  $|\bar{\sigma}_A| = |\bar{\sigma}_B| = 137.3 \text{ MPa}$ , which is close to the yield strength of steel 304 at  $T = 650^\circ\text{C}$ .

The test results showed that in the case  $\theta = 30^\circ$  immediately after the rotation of the stress tensor, the strain rate slightly increases. When rotated by  $90^\circ$ , there is a temporary increase in the rate of axial and



**Fig. 2.** Creep curves for Kh18N10T steel at a temperature of 850°C: (1)  $\sigma_{II} = 80$  MPa, (2)  $\sigma_{II} = 600$  MPa, (3)  $\sigma_{II} = 50$  MPa, (4)  $\sigma_{II} = 40$  MPa.

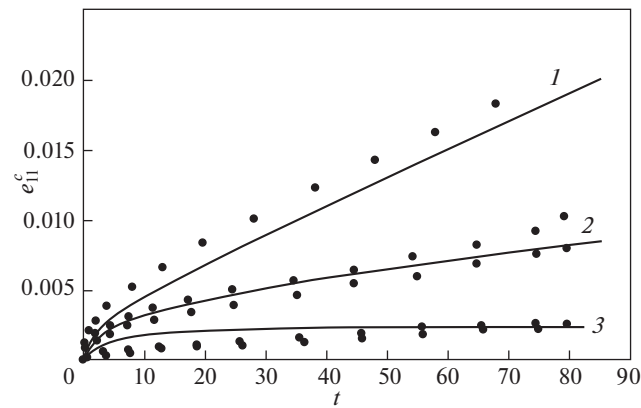


**Fig. 3.** Creep curves of steel 304 at a temperature of 650°C: (1)  $\sigma_{II} = 156.9$  MPa, (2)  $\sigma_{II} = 137.3$  MPa, (3)  $\sigma_{II} = 117.7$  MPa.

shear deformations after the change from tension to torsion and torsion to tension. This transient increase in strain rate decreases as the duration of cyclic loading increases.

At large angles of rotation of the stress vector  $\theta = 150^\circ$  and  $180^\circ$ , there is a noticeable temporary increase in the strain rate after each rotation of the stress vector, similar to that observed during the initial application of the load (Figs. 5–8). Thus, it can be concluded that the softening of the material after rotation of the stress vector becomes most pronounced with an increase in the angle of rotation.

Another essential feature of creep strains under complex loading is the non-collinearity of the stress vector and creep strain rates at the transitional stage immediately after the rotation of the stress vector.

#### 4. CONCLUSION

A mathematical model that describes the processes of non-stationary creep of structural materials under non-stationary complex loading has been developed.

The results of numerical simulation and experimental data of creep processes for Kh18N10T and 304 steels are compared. It is shown that the developed version of constitutive relations of unsteady creep allows one to describe creep processes of metals under uniaxial and multiaxial stress states with sufficient accuracy for engineering calculations.

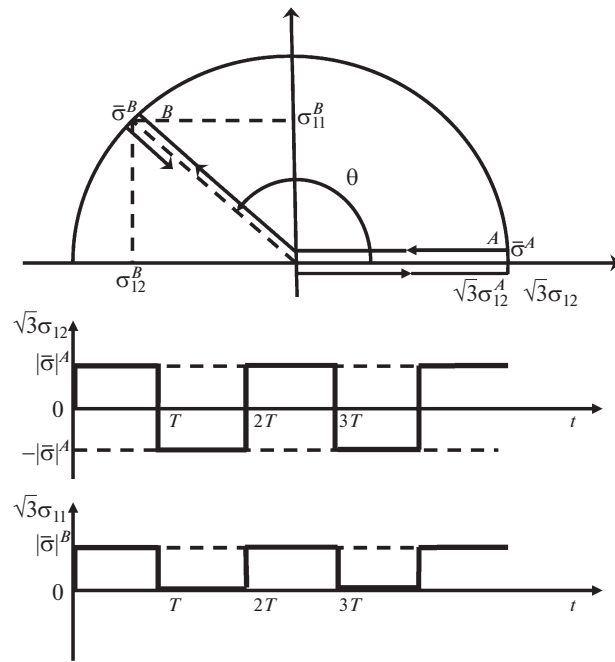


Fig. 4. Scheme of loading steel 304 during a creep test at a temperature of 650°C,  $T = 8$  h.

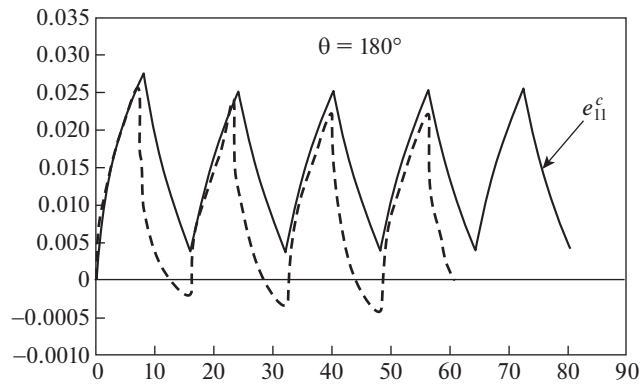


Fig. 5. Change in creep strain as a function of time at  $\theta = 180^\circ$ .

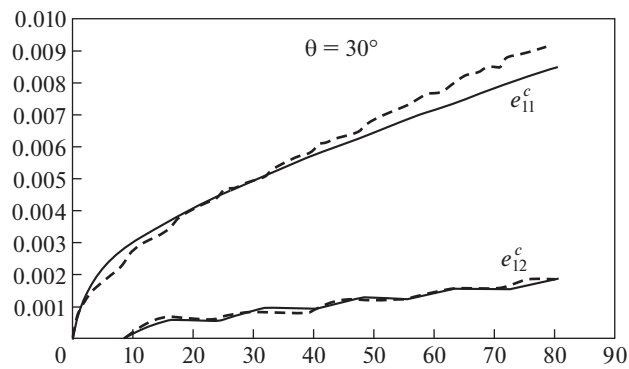


Fig. 6. Change in creep strains as a function of time at  $\theta = 30^\circ$ .

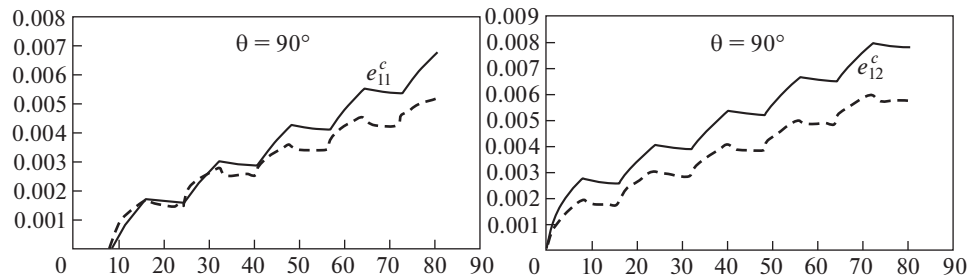


Fig. 7. Change in creep strain as a function of time at  $\theta = 90^\circ$ .

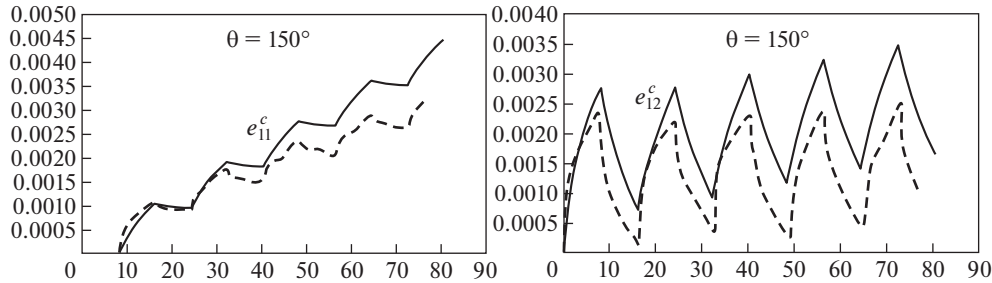


Fig. 8. Change in creep strain as a function of time at  $\theta = 150^\circ$ .

#### FUNDING

The study was supported by the Ministry of Science and Higher Education of the Russian Federation (project no. 0729-2020-0054).

#### REFERENCES

1. G. M. Khazhinskii, "On the theory of creep and long-term strength of metals," *Izv. AN SSSR Mekh. Tv. Tela*, No. 6, 29–36 (1971).
2. Yu. N. Rabotnov, "On the mechanism of gradual failure," in *Questions of Strength of Materials and Construction* (AN SSSR, Moscow, 1959), pp. 5–7.
3. N. N. Malinin, *Applied Theory of Plasticity and Creep* (Mashinostroenie, Moscow, 1968) [in Russian].
4. S. Savalle and G. Caienatd, "Microanureage, micropropagation et endommagement," *La Resherche Aerospaciale* 6, 395–411 (1982).
5. I. A. Volkov, L. A. Igumnov, and Yu. G. Korotkikh, *Applied Theory of Viscoplasticity* (Nizh. Novg. Gos. Univ., Nizhni Novgorod, 2015) [in Russian].
6. C. M. Stewart, "Tertiary creep damage modeling of a transversely isotropic Ni-based superalloy," in *Electronic Theses and Dissertations, 2004–2019* (Univ. of Central Florida, 2009), 4105.
7. Y. Ohashi, M. Kawai, and T. Kaito, "Inelastic behavior of type 316 stainless steel under multiaxial nonproportional cyclic stressings at elevated temperature," *J. Eng. Mater. Technol.* 107 (2), 101–109 (1985). <https://doi.org/10.1115/1.3225781>
8. A. M. Lokoshchenko, L. V. Fomin, W. V. Teraud, et al. "Creep and long-term strength of metals under unsteady complex stress states (Review)," *Vestn. Sam. Gos. Tekhn. Univ., Ser. Fiz.-Mat. Nauki* 24 (2), 275–318. <https://doi.org/10.14498/vsgtu1765>
9. V. P. Radchenko, M. N. Saushkin, and E. P. Goludin, "Stochastic model of nonisothermal creep and long-term strength of materials," *J. Appl. Mech. Tech. Phy.* 53, 292–298 (2012). <https://doi.org/10.1134/S0021894412020186>
10. I. A. Volkov, L. A. Igumnov, D. A. Kazakov, et al., "A damaged medium model for describing the process of long-term strength of structural materials (metals and their alloys)," *Probl. Prochn. Plastichn.* 79 (3), 285–300 (2017). <https://doi.org/10.32326/1814-9146-2017-79-3-285-300>



11. Hua-Tangandet Yao, "A review of creep analysis and design under multi-axial stress," Nucl. Eng. Des. **237**, 1969–1986 (2007).  
<https://doi.org/10.1016/j.nucengdes.2007.02.003>
12. A. M. Lokoshchenko, "Long-term strength of metals in complex stress state (a survey)," Mech. Solids **47**, 357–372 (2012).  
<https://doi.org/10.3103/S0025654412030090>
13. I. A. Volkov and L.A. Igumnov, *Introduction to the Continuum Mechanics of a Damaged Medium* (Fizmatlit, Moscow, 2017) [in Russian].
14. A. M. Lokoshchenko, *Creep and Long-Term Strength of Metals* (Fizmatlit, Moscow, 2016; CRC Press, Boca Raton, 2018).
15. I. A. Volkov, D. A. Kazakov, and Yu. G. Korotkih, "Experimental and theoretical methods for determining the parameters of equations of mechanics media failure for fatigue and creep," Vestn. PNIPU Mekh., No.2, 30–58 (2012).

*Translated by A.A. Borimova*